Geodesy and Geodynamics 2014,5(2):48-53

http://www.jgg09.com
Doi:10.3724/SP.J.1246.2014.02048

Preseismic deformation associated with the 2014 *Ms*7.3 Yutian earthquake derived from GPS data

Chen Changyun[1], Chen Fuchao[1], Zheng Zhijiang[1], Zhu Shuang[1], Zhang Junlong[2] and Yang Panxin[2]
[1]*First Crust Monitoring and Application Center, China Earthquake Administration, Tianjin* 300180, *China*
[2]*Institute of Earthquake Science, China Earthquake Administration, Beijing* 100036, *China*

Abstract: Based on analysis of the GPS data during 1999-2007, 2009-2011, and 2011-2013 mainly from the Crustal Motion Observation Network of China, we obtained the GPS horizontal velocity field, the GPS strain rate field, and the profiles across the southwestern segment of the Altyn Tagh Fault zone and its adjacent regions and identified the different characteristics of horizontal crustal deformation fields and profiles during different periods. The results show that, before the February 12, 2014, *Ms*7.3 Yutian earthquake, the laevorotation deformation along the southwestern segment of the Altyn Tagh Fault zone increased about 3.3 mm/a during 2011-2013, relative to that in 2009-2011, and the GPS strain rate field distributed in the southeastern segment of the Altyn Tagh Fault during 2011-2013 increased obviously. These abnormal changes may be regarded as precursors to the *Ms*7.3 Yutian earthquake.

Key words: Yutian earthquake; Altyn Tagh Fault; GPS; velocity field; strain field

1 Introduction

Fault interaction and earthquake occurrence have attracted considerable attention in the seismological community during recent years. It is known that temporal-spatial variations of crustal deformation fields affect the motion and deformation features of faults. An *Ms*7.3 earthquake occurred in Yutian County (36.1° N, 82.5°E), in the Xijiang autonomous region, China, on February 12, 2013, at a focal depth of 12 km. This earthquake occurred along the southwestern segment of the Altyn Tagh Fault zone, which is the boundary between two new tectonic landforms, the Tibetan Plateau and the Tarim Basin[1]. About 100 km to the southwest of the epicenter, on the same fault segment, another *Ms*7.3 earthquake had occurred on March 21, 2008. It is important to find out whether any information about the precursors of these two earthquakes can be obtained from GPS data, which can provide us with information on large-scale changes of crustal deformation easily.

Based on GPS data, in this study we analyze crustal deformation features in the southwestern segment of the Altyn Tagh Fault zone and its adjacent regions. To obtain the preseismic deformation field, and given the effects of the *Ms*7.3 Yutian earthquake in 2008, the GPS data used in this study were selected mainly from three periods: 1999-2007, 2009-2011, and 2011-2013. Emphasis is placed on the temporal and spatial variations of the crustal deformation field before February 12, 2014, combined with earthquake geology data.

2 Geologic setting and seismic activity

The Altyn Tagh Fault zone is located between the Tar-

Received:2014-03-15; Accepted:2014-04-04
Corresponding author: Chen Changyun, E-mail: ccy_666@163.com
This work is supported by the Spark Progoram of Earthquake Science (XH13037Y), Earthquake Tracking (2014010203), and the National Natural Science Fourdation of China (41372215,41272233,41174004).

im Basin to the northwest and the Tibetan Plateau to the southeast (Fig. 1). The active trace of the Altyn Tagh Fault is a well-defined morphologic feature between longitudes of 80°E and 95°E[2]. As one of major active tectonic features produced during the India-Asia collision, the Altyn Tagh Fault can be divided into two segments based on fault-trace geometry: a northern margin segment and a southern margin segment[3]. The northern margin segment of the Altyn Tagh Fault zone underwent a gradual change from compressional thrust through left-lateral strike slip simultaneously with compressional thrust to pure left-lateral strike slip[4]. The southern margin segment of the Altyn Tagh Fault zone trends NE, starting from Lapeiquan in the Altyn Mountains and ending at the southern margin of Alashan to the northeast, and is about 860 km long. Slip rates along the Altyn Tagh Fault during the Quaternary are fairly well known[1-5]. Based on geomorphic surveys of displaced fluvial and stream terraces and testing of ages, Xu et al[1] obtained a strike-slip rate for the southwestern segment of the Altyn Tagh Fault of about 17.5 ± 2 mm/a to the northeast. This rate decreased from 10± 2 mm/a in the middle part of the Altyn Tagh Fault zone to 1-2 mm/a along the northeasternmost of the fault[5]. The Altyn Tagh Fault is seismically active, with four large earthquakes (*M*s > 7.0) occurring along this fault since instruments were deployed to record seismic activity (Fig. 1): 2 large earthquakes (*M*s7.2 and *M*s7.3) along the west of Qiemo along the southwestern segment of the Altyn Tagh Fault zone in July, 1924[6,7], one on March 21, 2008[8], and the other on February 12, 2014.

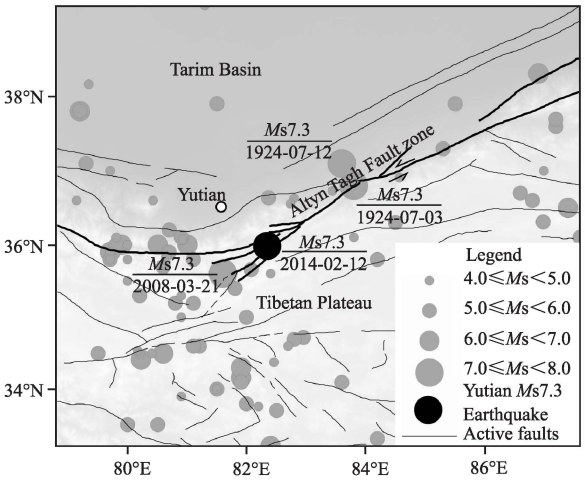

Figure 1 Active faults and seismicity in the southern segment of the Altyn Tagh Fault

3 Data acquisition and processing

The GPS data used in this study are mainly from the Crustal Motion Observation Network of China (CMONC) project. They mainly include data from regional survey mode stations operated in 1999, 2001, 2004, 2007, 2009, 2011, and 2013. GAMIT/GLOBK software version 10.40[9,10] and QOCA[11] software are utilized to analyze the GPS data. The data were processed in four steps[12,13]. For ease of interpretation, in this study we express velocities relative to the stable Eurasia plate (Fig.2). The Eurasia reference frame is realized by subtracting the rotation of the Eurasian plate from that of the ITRF2005. To study deformation in a boundary region that is wide and distant from the stable region of either adjoining plate, a more robust approach is to determine the frame by using stations within the stable interiors of the adjoining plates, thereby minimizing the velocities within each plate[14]. Accordingly, in this study, the estimated Eurasian plate

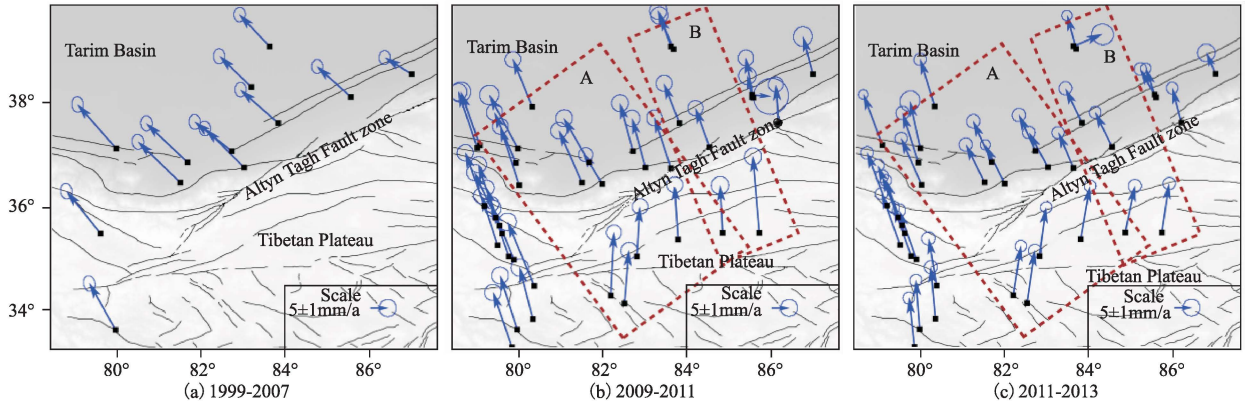

Figure 2 GPS velocity field at different times in the southwestern segment of the Altyn Tagh Fault

rotates at 0.261 ± 0.003 °/Ma, with a pole at 56.330° ± 0.549°N, 95.979° ± 0.969°E, which is obtained by Altamimi et al[15] based on analysis of data from GPS, very long baseline interferometry, and satellite laser ranging.

4 Horizontal crustal deformation fields

4.1 GPS horizontal velocity field

In figure 2, the horizontal velocities of GPS stations in a Eurasia-fixed reference frame clearly demonstrate the first-order characteristics of motion and deformation of the two tectonic units the Tarim Basin and the Tibetan Plateau, especially the remarkable motion in different directions on either side of the Altyn Tagh Fault zone. From southwest to northeast, the horizontal velocity decreased noticeably northwest of the Altyn Tagh Fault zone. With respect to horizontal velocities during 1999–2007, the results during 2009–2011 show that the velocities of GPS stations northwest of the Altyn Tagh Fault zone were deflected eastward. These deformation features were evident before and after the 2008 Wenchuan earthquake and may be affected by the postseismic deformation of the Wenchuan earthquake. Relative to the horizontal velocities during 2009–2011, the GPS velocities during 2011–2013 demonstrated that the velocities northwest of the Altyn Tagh Fault zone changed little, not only in direction but also in magnitude. However, the velocities southeast of the Altyn Tagh Fault zone show significant deflection from north to north-northeast, indicating possible left-lateral strike slip enhancement during 2009–2013. To better analyze the motion characteristics of the Altyn Tagh Fault zone, in this study we focus on the strike-slip rate of different segments of the Altyn Tagh Fault zone (Figs.3 and 4).

The dashed rectangular boxes in figure 2 show the location of GPS velocity profiles across the southwestern segment of the Altyn Tagh Fault zone in figures 3 and 4. Figures 3 and 4 represent the parallel and vertical components of GPS velocity profiles, respectively. The two profiles clearly demonstrate the temporal and spatial variations along the southwestern segment of the Altyn Tagh Fault zone.

In figure 3(GPS velocity profile A), the GPS velocity component parallel to the Altyn Tagh Fault during 2011–2013 clearly demonstrates that left-lateral strike slip increased from that occurring during 2009–2011, from 4.8 ± 0.9 to 8.1 ± 0.7 mm/a (an increase of about 3.3 mm/a). In figure 3(GPS velocity profile B), the GPS velocity component parallel to the Altyn Tagh Fault during 2011–2013 demonstrates that left-lateral strike slip during 2009–2011 increased too, from 6.9± 0.9 to 7.6 ± 0.8 mm/a (an increase of about 0.7 mm/a). Although the GPS velocity component vertical to the Altyn Tagh Fault during 2011–2013 on both sides of the fault decreased with respect to that during 2009–2011, crustal deformation reflected by the differential motion on either side of the Atlyn Tagh Fault is not obvious (Fig.4). The significant increases of GPS velocity parallel to the fault show that left-lateral strike slip played an important role in the motion of the Atlyn Tagh Fault. Along the southwestern segment of the Altyn Tagh Fault, compared with GPS velocity profile B, GPS velocity profile A demonstrates an obvious left-lateral strike slip, perhaps indicating segmentation and inheritance of the active fault. The left-lateral strike slip of GPS velocity profile A across the Altyn Tagh Fault increased significantly and this abnormal change may be regarded as a precursor to the February 12, 2014, *M*s7.3 Yutian earthquake.

4.2 Strain rate field from GPS velocity field

Analysis of the strain rate field based on the GPS data can allow us to monitor the temporal and spatial variations of crustal deformation. To get a continuous strain rate map of the southwestern segment of the Altyn Tagh Fault zone and its adjacent regions, we use a least-squares collocation technique to interpolate the GPS velocities on 0.5° × 0.5° (longitude and latitude) grids and then calculate the strain rate on the grids (Fig.5)[16]. As shown in figure 5, the strain rate along the southwestern segment of the Altyn Tagh Fault varies from place to place, exhibiting an uneven spatial distribution. For some regions along major active faults, the strain rate is several times higher than the average of the whole area. The strain rate along the Altyn Tagh Fault is dominated mainly by NE-trending principal compressive strain, accompanied by NW-trending principal tensile strain, and the amplitude of the latter is generally much smaller than that of the former. To gain

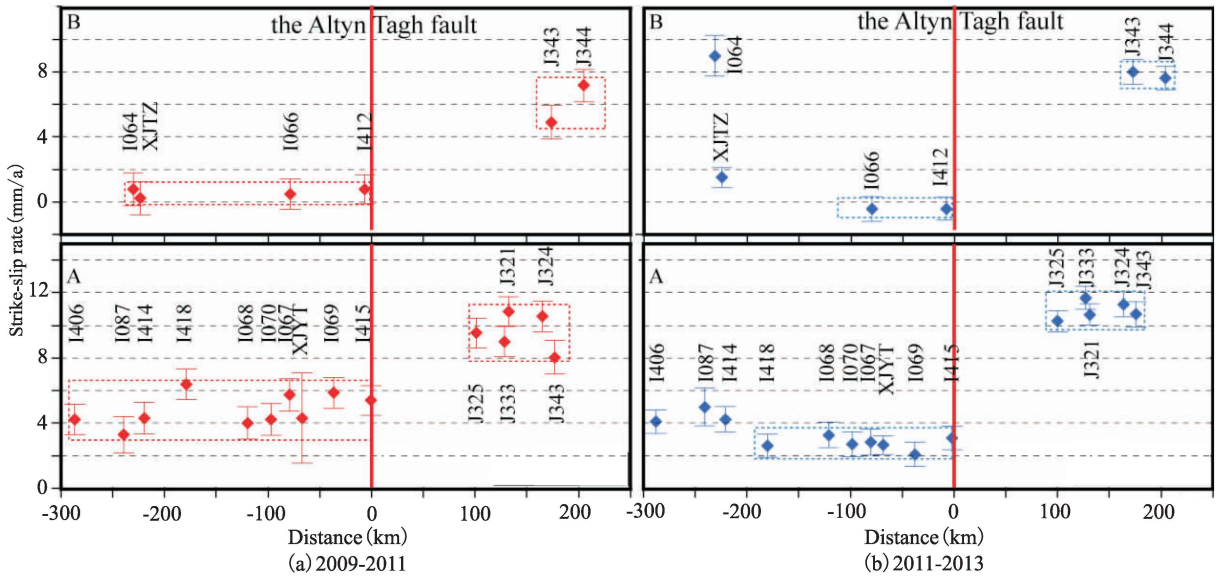

Figure 3 GPS velocity profiles across the southwestern segment of the Altyn Tagh Fault and parallel components with respect to the distance along the profile; data entries are indexed by the regions outlined in figure 2

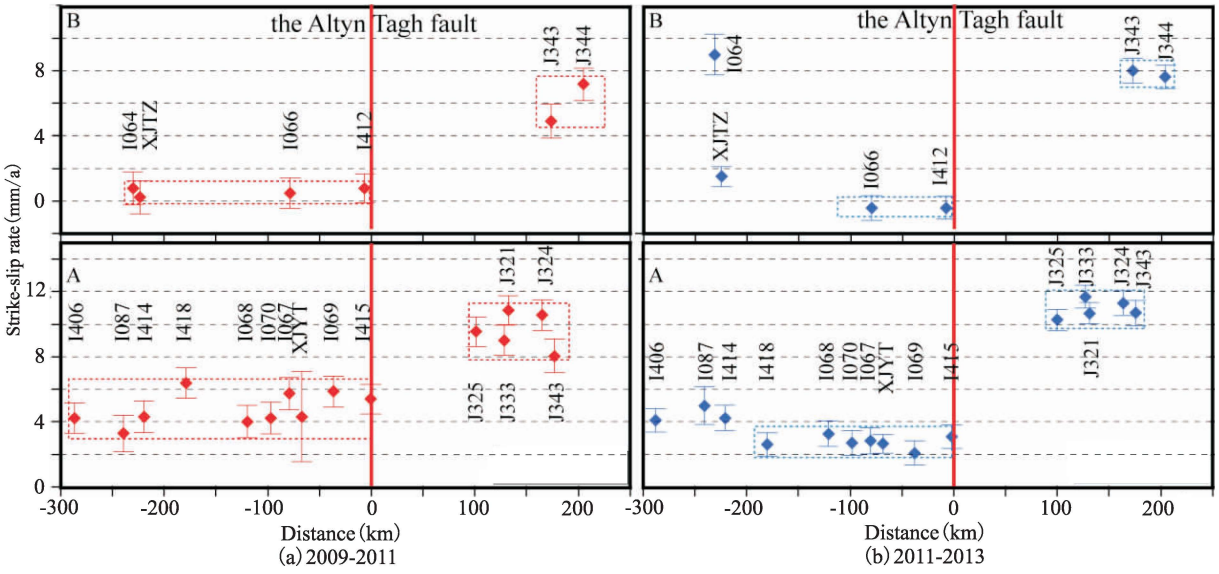

Figure 4 GPS velocity profiles across the southwestern segment of the Altyn Tagh Fault and vertical components with respect to the distance along the profile; data entries are indexed by the regions outlined in figure 2

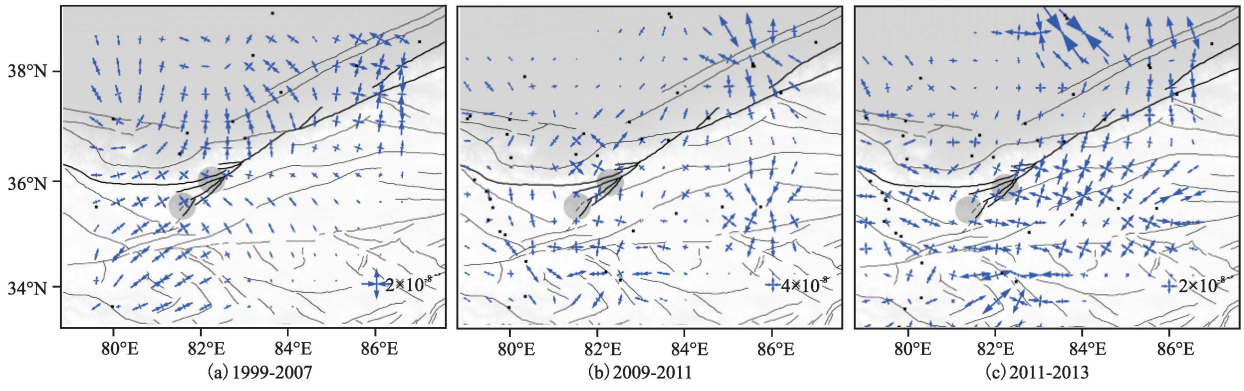

Figure 5 GPS principal strain rate field at different times in the southwestern segment of the Altyn Tagh Fault; GPS stations are indicated by black squares, and the gray circles indicate the 2008 and 2014 *Ms*7.3 Yutian earthquake, respectively

a better understanding of the strain rate in the research zone, we compared the change in the strain rate field on both sides of the Altyn Tagh fault and found that, from southwest to northeast extending along the trend direction of the Altyn Tagh Fault, the strain rate clearly increased. The angle between the direction of principal strain rate and the Altyn Tagh Fault trend may suggest that the fault underwent an obvious left-lateral shear deformation.

Based on analysis of the temporal and spatial variations of the strain rate field in the research zone as shown in figure 5, we found that the strain rate in the epicenter region of the 2008 *Ms*7.3 Yutian earthquake decreased after the earthquake and increased gradually before the 2014 *Ms*7.3 Yutian earthquake. The difference in strain rate features between the periods 1999–2007 and 2009–2011 show that differential motion on both sides of the Altyn Tagh Fault occurred, with strain rate clearly decreasing northwest of the Altyn Tagh Fault and increasing southeast of the fault. This latter increasing trend continued during the period 2011–2013, perhaps indicating that the research zone is in a high strain accumulation environment, a characteristic signifying high seismic risk.

5 Discussion and conclusions

Using GPS data obtained from 1999 to 2013, we have obtained the horizontal velocity field, the strain rate field, and the profiles across the southwestern segment of the Altyn Tagh Fault zone, respectively. Our results are summarized as follows:

1) On both sides of the southwestern segment of the Altyn Tagh Fault, the GPS velocities are not only different in direction but also in magnitude, indicating differential movement on the two sides of the fault. The GPS velocity component parallel to the Altyn Tagh Fault zone during 2011–2013 clearly demonstrates that left-lateral strike slip increased over that occurring during 2009–2011, from 4.8 ± 0.9 to 8.1 ± 0.7 mm/a (an increase of about 3.3 mm/a).

2) The strain rate along the southwestern segment of the Altyn Tagh Fault exhibits an uneven spatial distribution. During 1999–2007, the strain rate along the northwestern part of the fault is larger than that along the southeastern part. The difference in strain rate between 1999–2007 and 2009–2011 indicates that differential motion on both sides of the Altyn Tagh Fault is significant, with strain rate clearly decreasing northwest of the Altyn Tagh Fault and increasing southeast of the fault. The latter increasing trend continued during the period 2011–2013.

3) Temporal and spatial variations of the crustal deformation field show that the occurrence of the February 12, 2014, *Ms*7.3 Yutian earthquake may be related to the enhancement of left-lateral shearing along the Altyn Tagh Fault and the increases of strain rate in the southeastern part of the Altyn Tagh Fault.

Whether the GPS velocity profiles across the active faults and the strain rate field obtained by the least-squares collocation technique can be used as reliable indictors of earthquake precursors depends on several hypotheses. Given that the Altyn Tagh Fault zone is one of the boundary control faults located along the northern margin of the Tibetan Plateau, the GPS velocity profiles in this study can only be used to analyze the effects of the Altyn Tagh Fault-the effects of other secondary faults are neglected. The calculation of strain rate in this study is mainly based on the continuum hypothesis, without the complexity of the medium properties taken into account. In fact, the Altyn Tagh Fault zone is located between the Tarim Basin to the northwest and the Tibetan Plateau to the southeast, so differences of crustal media are great, and these differences will greatly influence the crustal deformation in the southwestern segment of the Altyn Tagh Fault zone and its adjacent regions.

References

[1] Xu X W, Wang F, Zheng R Z, et al. Late Quaternary sinistral slip rate along the Altyn Tagh fault and its structural transformation model. Sci. China. Ser. D: Earth Sci., 2005, 384–397.

[2] Peltzer G, Tapponnier P and Armijio R. Magnitude of the late Quaternary left-lateral displacements along the northern edge of Tibet. Science, 1989, 246: 1285–1289.

[3] Zheng Rongzhang. Tectonic uplift and deformation mechanism of the Altun structural system since the middle-late period of the Pleistocene time. Beijing, Institute of Geology, CEA, 2005, PhD Thesis. (in Chinese)

[4] Xing Chengqi, Zhang Jie and Lv D W. Discussion on change and its mechanism of movement forms of the active fault zone along

north margin of Mt. Altun. Northwest Seismol. J., 1998, 20(2): 52-57. (in Chinese)

[5] Zhang P Z, Molnar P and Xu X W. Late Quaternary and present-day rates along the Altyn Tagh Fault, northern margin of the Tibetan Plateau. Tectonics, 2007, 26, TC5010, doi: 10.1029/2006TC002014

[6] States Seismological Bureau of China (SSBC). The Altyn Tagh active fault system (in chinese). Beijing: Seismological Publishing House, 1992, 319 pp.

[7] Department of Earthquake Disaster Prevention, China Earthquake Administration, eds. The Catalogue of Chinese Historical Strong Earthquake. Beijing: China Science and Technology Press, 1999, 1-637. (in Chinese)

[8] China Earthquake Networks Center. http://www.csndmc.ac.cn/newweb/data.htm

[9] Herring T A, King R W and McClusky S C. GAMIT Reference Manual. GPS Analysis at MIT. Release 10.4. Massachusetts Institute of Technology, 2010, http://www-gpsg.mit.edu/~simon/gtgk/index.htm

[10] Herrring T A, King R W and McClusky S C. GLOBK Reference Manual. Global Kalman filter VLBI and GPS analysis program. Release 10.4. Massachusetts Institute of Technology, 2010, http://www-gpsg.mit.edu/~simon/ gtgk/index.htm

[11] Dong D, Herring T A and King R W. Estimating regional deformation from a combination of space and terrestrial geodetic data. J. Geophys. Res., 1998, 72:200-214.

[12] Gan W J, Zhang P Z, Shen Z K., et al. Present-day crustal motion within the Tibetan plateau inferred from GPS measurements. J. Geophys. Res., 2007, 112: B08416, doi:10.1029/2005JB004120.

[13] Wu Yanqiang, Jiang Zaisen, Wang Min, et al. Preliminary results of the co-seismic displacement and pre-seismic strain accumulation of the Lushan *Ms*7.0 earthquake reflected by the GPS surveying. China Sci. Bull., 2013, 58: 1910-1916, doi: 10.1007/s11434-013-5998-5. (in Chinese)

[14] Steblov, G M, Kogan M G, King R W, et al. Imprint of the North American plate in Siberia revealed by GPS. Geophys. Res. Lett., 2003, 30: 2041-2044.

[15] Altamimi Z et al. ITRF2005: A new release of the international terrestrial reference frame based on time series of station positions and earth orientation parameters. J. Geophys. Res., 2007, 112: B09401, doi:10.1029/2007JB004949.

[16] Wu Y Q, Jiang Z S, Yang G H, et al. Comparison of GPS strain rate computing methods and their reliability. Geophys. J. Int., 2011, 185: 703-717, doi:10.1111/j.1365-246X.2011.04976x.